

SOME ASPECTS TO THE FORMATION OF THE DROPLETEPITAXIAL III-V BASED NANOSTRUCTURES

Ákos Némcsics

*Institute for Microelectronics and Technology, Óbuda University, Tavaszmező u. 17. H-1084 Budapest, Hungary; and Institute for Technical Physics and Materials Science, Natural Sci. Res. Centre, Hungarian Academy of Sciences, P.O.Box 49. H-1525 Budapest, Hungary,
E-mail: nemcsics.akos@kvk.uni-obuda.hu*

Received 29 April 2013; accepted 07 May 2013

1. Introduction and Experimental Preliminaries

The low dimensional structures, grown by molecular beam epitaxy (MBE), has revolutioned the electronic devices both in their potentials and efficiency. Nowadays, the growth of self-assembled nanostructures has been intensively investigated for basic physics and device applications. It is very important to understand their growth kinetics and to know their shape. For a long time, for zero dimensional system production, the strain-induced method, based on the lattice mismatch, was the only known process.

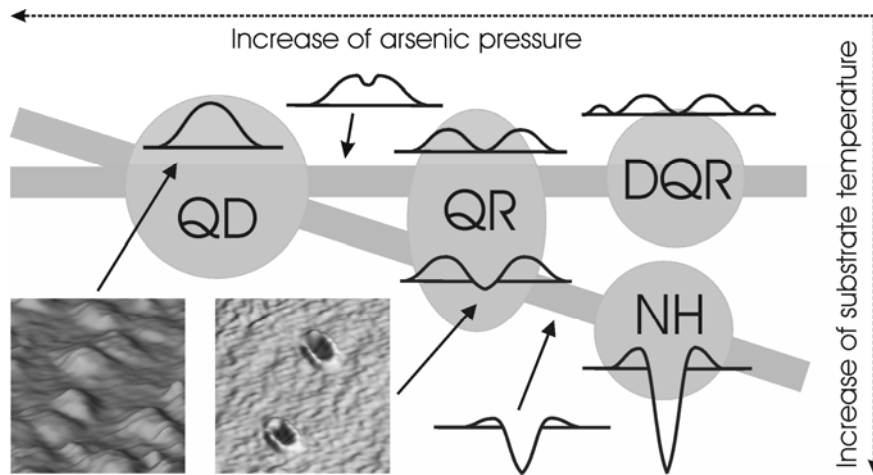


Fig. 1: *The shape of the droplet epitaxially grown nanostructure can be tuned by the technological parameters. Overview of the III-V based droplet epitaxially grown nanostructures such as quantum dots (QDs), quantum rings (QRs), double quantum rings (DQRs) and nano holes (NHs).*

Based on Koguchi's discoveries, a droplet epitaxial technique evolved, giving greater opportunities for the development of the self-organising nanostructures [1,2]. In this method, the lattice-mismatch lost its significance and with the new procedure, it is possible to create quantum dots (QDs) [3-7], quantum rings (QRs) [8-10], double quantum ring (DQRs) [11, 12] as well as nano holes (NH) (Fig. 1.) [13-15]. The electronic structure of these nanoobjects depend very much on their shape. Roughly, the droplet epitaxial process is the following: first, metal (e.g. Ga) droplets are generated on the surface in the Volmer-Weber-like growth mode. After, the crystallization of the droplets and their transformation into e.g. GaAs QDs under arsenic pressure. In order to control the process it is necessary to understand the kinetics of the growth process. Here, no theoretical description is available yet of the

underlying growth mechanism. Here, we are dealing with the III-V based structures. The forms of the GaAs nanostructures, grown on AlGaAs (001) substrate, is strongly dependent on the applied technology.

Here, the technological parameters of five different nanostructures are given. Later, the formation kinetics of these nanostructure are qualitatively discussed. The solution process investigated at two cases. The NHs (sample i) was generated at 570 °C in AlGaAs surface applying 6.4 ML Ga [14]. In this case, The AFM measurement shows NHs and very large clusters [14]. The next nanostructure (sample ii) was prepared similarly, but the Ga coverage was different (3.2 ML) [13,14]. Here, the AFM picture shows deep NHs surrounded by ring like bulge formations and shallow NHs, with plane rims (without any bulge) [13,14]. The crystallization process is investigated at three samples. The first structure is QD (sample iii). The crystallization of the Ga droplet occurs during the high arsenic supply (2.5×10^{-4} Torr) at 150 °C [6]. The elemental map of TEM shows, that the QD had Ga inclusions [6]. The next sample (iv) is crystallized at 2×10^{-6} Torr arsenic pressure at low temperature (200 °C) [11]. We received DQR [11]. The last sample (v) is crystallized at about the same arsenic background (1.1×10^{-6} Torr) but at high temperature (500 °C) [15]. The middle of the structure is surrounded by single ring like bulge formations [15]. For detailed technological parameters of the above samples see the given references.

2. Discussion

We attempt to give a consistent explanation for the growth of the nanostructures, a mentioned earlier. As widely known, the properties in nano region differ from the bulk properties. Generally, the nano-properties are unknown and only the tendency of the change is established, relative to the bulk properties. Usually the starting and the end states are known. The explanation of the final process comes from the coherent explanations of the component processes. These process explanations are coherent and consistent only, when they describe the growth of a large number of different kind of nano-structures. It becomes only then consistent.

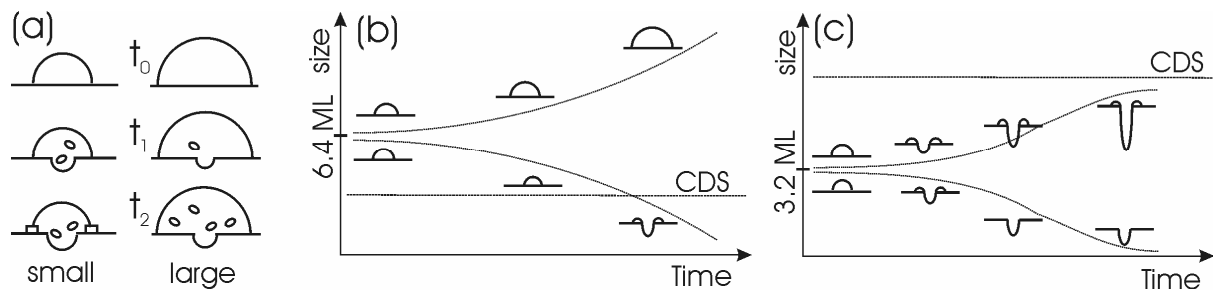


Fig. 2: (a) Explanation of the process 2 (see text); (b) Explanation of the temporal differentiation and solution process in case of large amount of deposited Ga (6.4 ML) [14] (see text); (c) Explanation this process at small Ga amount (3.2 ML) [13,14] (see text); where CDS means critical droplet size

After the deposition of Ga, part of the deposited Ga will combine with the surface arsenic atoms and the rest will form droplets. In order to form droplets at this temperature, the Ga atoms must migrate (process 1) on the GaAs and the Ga surfaces. It is well known, that with diminishing size the melting temperature is dropping and saturation concentration increases. This describes our present Ga droplets well (process 2) (this is the dominant process in cases of complete lack or in the presence small quantities of arsenic). It is also well known that, the crystallization starts at three-phase-line, when the conditions became favourable. In our case, this starts in line of the rim of the droplet (process 3). It is noted, that

the excess arsenic incorporates into the GaAs epitaxy when the temperature is low (about 300 °C or lower), creating stress in the lattice. (In presence of larger quantity of arsenic, these are the dominant processes).

Process 1 makes possible the phenomenon called Ostwald ripening. At the same time process 2 causes the difference between QD-s, QR-s and NH-s. Due to this process at the same temperature and during the same time the hole originated under the smaller droplets is deeper then under the larger droplets (Fig 2./a.). (That is supposing the time duration is not too long to run out of the material from the smaller droplets.) These findings are justified by the two experiments, where the deposited Ga quantity was 6.4 ML (Fig 2./b) and 3.2 ML (Fig. 2./c), respectively. At a given temperature there is a critical droplet size under which the solution begins. After the Ga deposition, droplets form, followed by the growth of the larger droplets in the expense of the smaller ones. When the critical size is reached, the substrate solution by the droplet begins. We start with investigating the case of Ga 6.4 ML [14]. During the experiment, the formation of small NH-s and large QD-s can be observed (sample i) [14]. We can follow the process on Fig. 2./B, where large quantity of Ga deposited. The sizes of the droplets formed, are above the critical size. After the deposition starts the differentiation of the droplets. The smaller droplets reach the critical size and start solving the substrate. This state is frozen by the opening the arsenic cell.

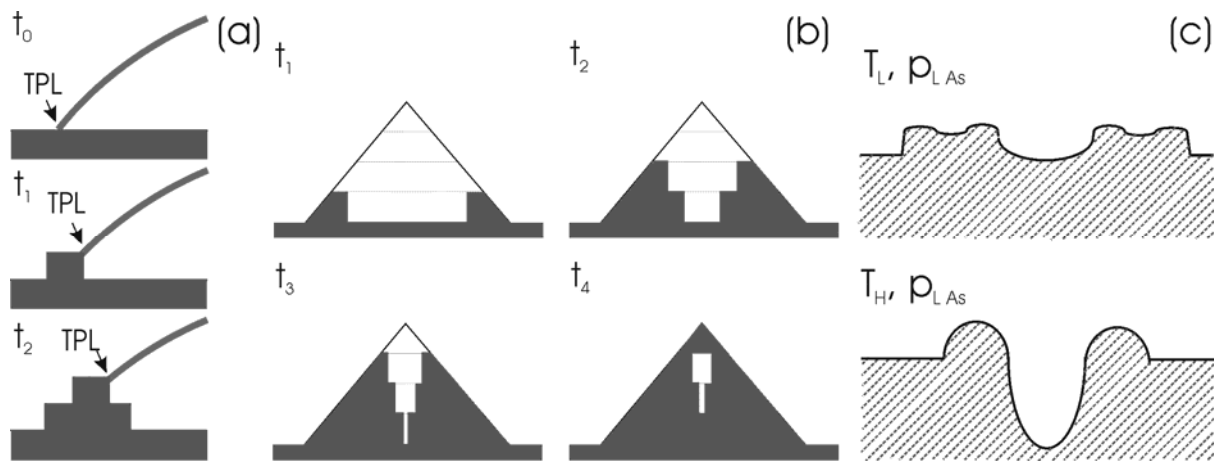


Fig. 3: (a) Explanation of the crystal seed formation at the droplet rim (see text). (b) Explanation of the formation of Ga inclusion inside of the QD ($T_{sub} = 150 \text{ }^\circ\text{C}$, $p_{As} = 2.5 \times 10^{-4} \text{ Torr}$) [6] (see text); (c) upper part: cross section of a DQR ($T_{sub} = 200 \text{ }^\circ\text{C}$, $p_{As} = 2.6 \times 10^{-6} \text{ Torr}$) [11]; lower part cross section of a NH ($T_{sub} = 500 \text{ }^\circ\text{C}$, $p_{As} = 1.1 \times 10^{-6} \text{ Torr}$) [15]; where TPL means three-phase-line

The second case is when the deposited Ga is 3.2 ML [13,14]. Here, we can observe shallow NHs, with plane rims (without any bulge), and deep NHs surrounded by ring like bulge formations (sample ii) [13,15]. The explanation is given in Fig.2/c. In this case, the quantity of the deposited Ga is small. The formed droplets are under the critical size, therefore the solution starts under the droplets. Under the small droplets the solution is faster, but the material is used up in a short time. The reduction in material is due first to the solution and second to the material's migration towards the larger droplets. After a short time at the smaller droplets the solution stops, whilst it carries on further under the larger ones. The larger droplets will not be spent, therefore the surrounding ring will freeze after opening the arsenic cell.

Due to the 3rd process the crystallization originates at the rim of the droplets. At lower temperature the excess arsenic incorporates into the lattice. The interstitial arsenic

migrates towards the inside of the structure, reducing the lattice stress. A new interface is created in the inner and upper regions of the crystal centres. The growth of these centres are propagating in those directions (Fig. 3./a). The arsenic is fed from the outer surface of the structure. It was observed, that when the arsenic quantity was large the QD had Ga inclusions (sample iii) [6]. Its origin is explained above. The growth in height is similar to that of the basic circle; so the speed of growth in height is a linear function. The speed of growth towards the inner regions is accelerating, because assuming constant arsenic absorbing surface, the concentric area is diminishing with the reduced radius going towards the centre. The presence of the excess arsenic at lower temperature, is the explanation for the formation of the DQRs. The migration and the crystallization of the Ga would result in the creation of a larger ring (upper part of Fig. 3/c, sample (iv)) [11]. Instead, in excess to the original ring we end up with a second ring and this limiting effect on the size of the area is the result of the elimination of the lattice stress. The creation of DQRs can only be observed at lower temperature. At higher temperature DQRs cannot be created because arsenic is not incorporated in the lattice, which causes the stress in the lattice (lower part of Fig.3./c, sample (v)) [15].

Acknowledgement

This work was supported by the Országos Tudományos Kutatási Alap (OTKA), Grant Nos K75735 and K77331.

References:

- [1] N. Koguchi, S. Takahashi, T. J. Chikyow; *J. Cryst. Growth* **111** (1991).
- [2] N. Koguchi, K. Ishige; *Jpn. J. Appl. Phys.* **32** 2052 (1993).
- [3] T. Mano, K. Watanabe, S. Tsukamoto, H. Fujikoa, M. Oshima, N. Koguchi; *Jpn. J. Appl. Phys.* **38** L1009 (1999).
- [4] J. M. Lee, D. H. Kim, H. Hong, J. C. Woo, S. J. Park; *J. Cryst. Growth* **212** 67 (2000).
- [5] Ch. Heyn, A. Stemmann, A. Schramm, H. Welsch, W. Hansen, Á. Nemcsics; *Appl. Phys. Lett.* **90** 203105 (2007).
- [6] T. Mano, K. Mitsuishi, Y. Nakayama, T. Noda, K. Sakoda; *Appl. Surf. Sci.* **254** 7770 (2008).
- [7] Á. Nemcsics, L. Tóth, L. Dobos, Ch Heyn, A. Stemmann, A. Schramm, H. Welsch, W. Hansen; *Superlatt. Microstr.* **48** 351 (2010).
- [8] T. Mano, N. Koguchi; *J. Cryst. Growth* **278** 108 (2005).
- [9] T. Kuroda, T. Mano, T. Ochiai, S. Sanguinetti, K. Sakoda, G. Kido, N. Koguchi; *Phys. Rev. B* **72** 205301 (2005).
- [10] Á. Nemcsics, Ch. Heyn, A. Stemmann, A. Schramm, H. Welsch, W. Hansen; *Mat. Sci. Eng. B* **165** 118 (2009).
- [11] S. Sanguinetti, M. Abbarchi, A. Vinattieri, M. Zamfirescu, M. Gurioli, T. Mano, T. Kuroda, N. Koguchi; *Phys. Rev. B* **77** 125404 (2008).
- [12] T. Kuroda, T. Mano, T. Ochiai, S. Sanguinetti, T. Noda, K. Kuroda, K. Sakoda, G. Kido, N. Koguchi; *Physica E* **32** 46 (2006).
- [13] Ch. Heyn, A. Stemmann, W. Hansen; *J. Cryst. Growth* **311** 1839 (2009).
- [14] Ch. Heyn; *Phys. Rev. B* **83** 165302 (2011).
- [15] Zh. M. Wang, B. L. Liang, K. A. Sablon, G. J. Salamo; *Appl. Phys. Lett.* **90** 113120 (2007).